Revista Mexicana de Astronomía y Astrofísica, **43**, 179–189 (2007)

THE KINEMATICS OF ARP 295 IN Hα EMISSION: AN INTERACTING GALAXY WITH HIGHLY ASYMMETRIC ROTATION

Nathan Roche[1]

Instituto de Astronomía
Universidad Nacional Autónoma de México, Ensenada, B. C., Mexico

Received 2006 October 16; accepted 2006 December 11

RESUMEN

Investigamos Arp 295, un par de galaxias espirales interactuantes con $z = 0.023$, mediante espectroscopía óptica, imágenes en Hα y un mapeo de velocidad en Hα con el espectógrafo Echelle de Manchester. Las escalas de distancia son $r_{exp} = 5.24$ para Arp 295a y 2.52 kpc para 295b. Una galaxia Im mucho menor, Arp 295c, está asociada con la espiral mayor. Arp 295b es asimétrica; su disco está más extendido hacia el este pero las regiones de formación estelar más brillantes están en su lado oeste. El espectro de Arp 295b muestra fuertes líneas de emisión con una anchura equivalente de 36Åen [OII]3727. La luminosidad total en Hα de Arp 295b y Arp 295c es de 4.69×10^{41} y 6.76×10^{40} ergs s^{-1}, que corresponden a tasas de formación estelar de 3.7 y 0.53 $M_{\odot}$ año^{-1}. Para Arp 295b, medimos que la máxima velocidad de rotación del disco es de 252.6 ± 9.9 km s^{-1} y encontramos que la curva de rotación es muy asimétrica. El lado este (que se acerca a nosotros) tiene una velocidad radial mayor que el lado oeste; la máxima diferencia es de 88 km s^{-1} (en $r = 5$ arcsec), osea, un factor de 1.675.

ABSTRACT

We investigate Arp 295, a pair of interacting spirals at $z = 0.023$, using optical spectroscopy, Hα imaging, and Hα velocity mapping with the Manchester Echelle Spectrograph. Scalelengths are $r_{exp} = 5.24$ for Arp 295a and 2.52 kpc for 295b. A much smaller Im galaxy, Arp 295c, is associated with the larger spiral. Arp 295b is asymmetric with the disk more extended eastwards but with the brightest star-formation regions on its western side. The spectrum of Arp 295b shows strong emission lines with [OII]3727 equivalent width 36Å. The total Hα luminosities of Arp 295b and Arp 295c are 4.69×10^{41} and 6.76×10^{40} ergs s^{-1}, corresponding to star-formation rates 3.7 and 0.53 $M_{\odot}$ yr^{-1}. For Arp 295b, we measure the maximum disk rotation velocity as 252.6 ± 9.9 km s^{-1} and find the rotation curve is very asymmetric. The east (approaching) side has a higher radial velocity than the west with the maximum difference (at $r = 5$ arcsec) of 88 km s^{-1}, or a factor 1.675.

Key Words: **GALAXIES: INTERACTIONS**

1. INTRODUCTION

Arp 295, listed in the catalog of Arp (1966) as a 'double galaxy with long filaments', consists primarily of two interacting spiral galaxies: the south-western, Arp 295a, is a nearly edge-on (inclined 85°) Sc-type, the north-eastern, Arp 295b is an inclined (55°) Sb/peculiar/HII. There are visible tidal features – a luminous bridge connecting the two galaxies, a long luminous tail extending further SW from 295a, and a broad plume extending eastwards from Arp 295b.

Arp 295a is at RA $23^h41^m47^s.3$, Dec -03:40:02 and Arp 295b lies 4.59 arcmin away at RA $23^h42^m00^s.8$, Dec -03:36:55. The redshifts (recession velocities) are given by de Vaucouleurs et al. (1991) as $z = 0.022846$ (6849 ± 20 km s^{-1}) for 295a and $z = 0.023239$ (6967 ± 20 km s^{-1}) for 295b, greater

[1] Now at SAAO, South Africa.

by 118 ± 28 km s^{-1}. For $H_0 = 70$ km s^{-1} (assumed throughout this paper), the proper distance is 99.1 Mpc, the distance modulus 35.031 mag, and 1 arcsec will subtend 469.7 pc.

Stockton (1974) obtained long-slit spectra for the two galaxies, measured their radial velocity difference as 100 ± 20 km s^{-1}, found Arp 295b to be rotating in the sense that it is receding on its western side, and that Arp 295a is receding on its north-eastern side. Thus, with respect to their mutual orbit, Arp 295b rotates retrograde and Arp 295a prograde. Stockton found maximum rotation velocities (inclination-corrected) of 300 km s^{-1} for Arp 295a (with a turnover at $r = 40$ arcsec) and 245 km s^{-1} for Arp 295b (turnover at $r = 17$ arcsec), estimating from this that the 295a component is ~ 3.5 times more massive. However, their B-band magnitudes are almost the same, $B = 14.50/14.60$ for Arp 295a/b (de Vaucouleurs et al. 1991).

Arp 295 forms the first (earliest stage) in the sequence of mergers studied optically and in HI by Hibbard & van Gorkom (1996). They give far infra-red luminosities of 4.69×10^{43} ergs s^{-1} 295a and 3.83×10^{44} ergs s^{-1} for 295b, which from the relation of Kennicutt (1998), correspond to star-formation rates (SFRs) of 2.1 and 17.2 $M_{\odot}$yr^{-1}. They find that the more active Arp295b is also more gas-rich than the larger galaxy, with $M_{HI} \simeq 1.69 \times 10^{10}$ $M_{\odot}$ compared to 4.9×10^9 $M_{\odot}$.

Dopita et al. (2002) measure a Hα flux of 3.13×10^{-13} ergs cm^{-2} s^{-1} for Arp 295b, which corresponds to $L_{H\alpha} = 3.85 \times 10^{41}$ ergs s^{-1}, and from the relation of Kennicutt (1998), SFR $= 7.9 \times 10^{-42} L_{H\alpha}$, a SFR of 3.04 $M_{\odot}$yr^{-1}. Most of the Hα emission is from a number of 'knots' within the galaxy disk, with fainter ring-shaped emission to the north and south. From the far infra-red luminosity they derive a much higher SFR of 22.8 $M_{\odot}$yr^{-1} and account for the difference as dust extinction.

Neff et al. (2005), using GALEX data, detected UV emission from two small clumps within the gas-rich eastern plume of Arp 295b, about 90 arcsec ENE of the nucleus. These have very blue UV-optical colours, suggesting stellar ages $\sim 10^7$, and it was speculated that they could be formative tidal dwarf galaxies, each containing $\sim 10^6$ $M_{\odot}$ of stars but $\sim 10^8$ $M_{\odot}$ of gas.

Keel (1993) studied the kinematics of a sample of interacting pairs of spirals and found an association between kinematic disturbance, in the form of unusually low rotation velocities, and triggered star-formation. In this paper, we study kinematics and star-formation in the Arp 295 system by means of optical spectroscopy, deep imaging in Hα, and high-resolution spectroscopy of the Hα line with the Manchester Echelle Spectrograph (MES).

In Section 2 we describe our observations and data reduction. In Section 3 we present and interpret the optical spectroscopy, and in Section 4 the direct imaging in Hα. In Section 5 we use the Hα echelle spectroscopy to derive a velocity map and rotation curve. In Section 6 we summarize and discuss the effects of the galaxy interaction as revealed in our data.

2. OBSERVATIONS AND DATA

2.1. *Observations at OAN-SPM*

All observations were carried out at the Observatorio Astronómico Nacional, in the Sierra San Pedro Mártir, Baja California, México. The optical spectroscopy was performed on the night of 14 August 2005, using the 'Bolitas' spectrograph on the 0.84-m telescope. This small Boller and Chivens spectrograph was fitted with a Thompson 2k CCD (operated with 2×2 binning to give a 1024×1024 pixel image), an RGL grating set at an angle of approximately 6° to cover 3600Å$\leq \lambda \leq$ 5920Å, and a slit of width 160μm aligned E-W. To obtain a relative flux calibration we observed (through the same slit) the spectrophotometric standard star 58 Aquilae (Hamuy et al. 1994). For wavelength calibration, spectra were taken of a HeAr arc lamp.

Due to weather conditions and other difficulties we obtained usable spectra for only the more active galaxy, Arp 295b, consisting of 6×1200s exposures.

Our observations in Hα (restframe λ=6562.801Å in air) were performed on the nights of 15–18 August 2005, using the Manchester Echelle Spectrograph (MES) on the 2.1-m telescope. The MES (Meaburn 2003) is designed to obtain spatially-resolved profiles of individual emission lines, from faint extended sources such as nebulae and galaxies. It achieves high spectral/velocity resolution ($> 10^5$) and throughput by operating in a high spectral order with a narrow-band filter but no cross-disperser.

MES is fitted with a SITe3 CCD, which was operated with 2×2 binning to give a 512×512 pixel image of pixelsize 0.62 arcsec. The gain is $1.27e^{-1}$/ADU and we measure the readout noise as 12.35 ADU. At the redshift of Arp 295b, Hα is redshifted to 6715Å, where it falls near the centre (where sensitivity is greatest) of the echelle's 89th order. To isolate the redshifted Hα we observed through the E6690 filter, with width 91Å.

Three types of observation were taken with MES. Firstly, the instrument was used in direct-imaging mode – a mirror is inserted to bypass the slit and grating and image directly onto the CCD. The effective field of view is approximately 5.3×4.1 arcmin, so separate pointings are required for Arp 295a and 295b. In E6690, we obtained 5×1200s exposures of Arp 295b and one 1200s exposure of Arp 295a. For flux calibration, direct imaging was taken of the faint spectrophotometric standard star BD+33 2642 (Oke 1990).

Secondly, observation were taken though the slit and grating, to obtain a high-resolution profile of the Hα emission line at all points on the target galaxy along the slit. The slit, of width 150μm, was aligned E-W, and a total of 9×1200s exposures were taken on Arp 295b. The slit was moved slightly in the N-S direction between each exposure, so to cover 9 positions from the north to the south edge of the galaxy disk. Several further 1200s exposures were taken with the slit on Arp 295a or on other objects. Immediately before every exposure in spectroscopic mode, a 60 second 'mirror-slit' image was taken, which shows the slit position superimposed on a direct image of the galaxy, and a Th-Ar arc lamp exposure was taken for wavelength calibration.

Thirdly, exposures were taken through the grating with an open aperture instead of a slit, one of 1200s on each of Arp 295a and 295b. In this mode the Hα line will be 'smeared' by the extent of the galaxy in the dispersion direction. The motivation for this is that the integrated, background-subtracted flux in the slitless Hα line profile will give the total Hα flux of the galaxy without contamination from the red continuum. For flux calibration a slitless spectrum was taken of (again) 58 Aquilae.

2.2. *Data Reduction: 'Bolitas'*

The 'Bolitas' spectroscopic data were debiased and flat-fielded. Twilight sky flats were taken through the same slit/grating configuration as used for the observations. In the flat-fielding of spectroscopic data the aim is to remove the pixel-to-pixel sensitivity variations but not the variation along the wavelength direction. To do this, each pixel of the sky-flat was divided by the average value in its column (i.e. of all pixels at the same wavelength, averaged along the slit length), to produce a normalized flat-field with all wavelength dependence removed.

Calibration spectra of 58 Aquilae were spatially registered and combined, the 1D spectrum extracted (using IRAF 'apall'), wavelength-calibrated, and, with the tabulated spectral energy distribution for this star (Hamuy et al. 1994), used to derive a sensitivity (relative flux calibration) function. Our 6×1200s exposures of Arp 295b were spatially registered and combined (with 'sigclip' cosmic-ray rejection), then the 1D spectrum was extracted, wavelength calibrated, and flux calibrated in relative F_λ.

2.3. *Data Reduction: MES*

All the data were debiased. The twilight flats in direct-imaging mode were combined and normalized to give a master sky-flat for each observing night. All direct imaging and spectroscopic observations were then divided by the flat-field for their night of observation.

The flux of our calibration standard BD+33:2642 was measured using IRAF aperture photometry. From the tabulated spectral energy distribution of Oke (1990), the AB magnitude in the E6690 filter wavelength range is 11.080. We derive a zero-point for our E6690 direct-imaging of $21.209 - 0.089X$, where X is the airmass. A further correction is required for Galactic extinction at these co-ordinates - according to the Caltech NED, 0.102 mag at 0.65μm and 0.165 mag in the B band. We use this value but note that it could be an overestimate as Burstein & Heiles (1982) estimate extinction almost a factor of 2 smaller. This gives a zeropoint 20.981 for our combined observations of Arp 295b, and 20.998 for Arp 295a.

Our 5×1200s direct-imaging exposures of Arp 295b were spatially registered, sky subtracted, and combined, with 'sigclip' cosmic-ray removal. This was not fully effective in removing all cosmic rays, so an additional cleaning was performed with IRAF 'crmedian'. Our single 1200s exposure of Arp 295a was simply sky-subtracted and cleaned with 'crmedian'.

The spectroscopic mode MES images were also cleaned with 'crmedian'. and each was wavelength calibrated with the associated ThAr arc (we identified the lines with the NOAO spectral atlas). We find that our observations cover the range 6693.9 to 6745.7Å with a dispersion 0.1014Å pixel^{-1}. From our slitless spectrum of 58 Aquilae and the tabulated spectral energy distribution of Oke (1990), we derived an absolute flux calibration, which indicated the sensitivity of MES in our configuration to peak at 6725.5Å and vary by ≤ 0.5 mag over the observed λ range.

3. OPTICAL SPECTROSCOPY

Figure 1 shows the optical spectrum of Arp 295b, from 7200s of observation with 'Bolitas'. The galaxy is bright in the UV and has strong emission lines, especially [OII]3727, indicating high star-formation activity. The spectrum is plotted with only a relative flux calibration, as the slit will capture only

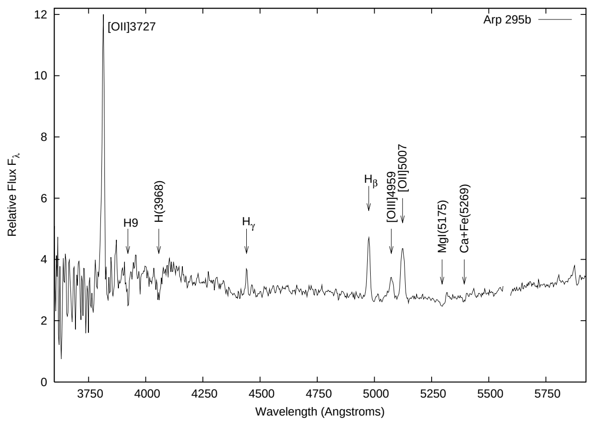

Fig. 1. Observed spectrum of Arp 295b, from 7200s of ‘Bolitas’ data (6 exposures), detected lines labelled.

TABLE 1

Line	EW Å (restframe)	Flux (10^{-14} ergs cm^{-2}s^{-1})
[OII]3727	36.4 ± 2.1	34.9 ± 2.0
H9(3835.4)	3.1 ± 1.3	-
H(3968.5)	3.2 ± 0.9	-
Hγ	3.0 ± 0.4	2.6 ± 0.3
Hβ	10.7 ± 0.4	9.2 ± 0.3
[OIII]4959	4.3 ± 0.4	3.7 ± 0.3
[OIII]5007	11.1 ± 0.5	9.7 ± 0.5
MgI(5175.4)	1.1 ± 0.4	-
Ca+Fe(5269)	0.8 ± 0.3	-

a fraction of the flux from the galaxy. However, if it is assumed that the region covered by the slit is representative of the whole galaxy, we can estimate an approximate absolute calibration by integrating the observed spectrum over a standard B-band response function and equating to the total magnitude $B \simeq 14.50$, which is $F_\lambda \simeq 9.53 \times 10^{-15}$ ergs cm^{-2} s^{-1}. In this way we estimate that one flux unit on Figure 1 corresponds to a flux from the whole galaxy of 3.10×10^{-15} ergs cm^{-2} s^{-1} Å^{-1}, and a luminosity of 3.82×10^{39} ergs s^{-1} Å^{-1}.

From our spectrum we calculate the B-band k-correction as 0.013 magnitudes. Using this, the absolute magnitude is $M_B = -20.44$.

Examining the spectrum we find 5 significant emission lines and 4 absorption lines. From the wavelengths of the emission lines we derive a redshift $z = 0.02322 \pm 0.00005$, or a recession velocity 6961 ± 15 km s^{-1}, in close agreement with de Vaucouleurs et al. (1991).

An error function $\sigma(\lambda)$ was estimated from the scatter between spectra separately extracted from each of the 1200s exposures. At $\lambda >$4500Å the detection of the continuum in each pixel is $\sim 20\sigma$. The error for each line’s width/flux measurements was estimated by summing $\sigma(\lambda)$ in quadrature over the line’s FWHM of 14Å.

Table 1 lists the detected lines with equivalent widths, measured using IRAF ‘splot’ and corrected to restframe (by dividing by $1 + z$), and for emission lines, fluxes estimated using the above calibration (not corrected for Galactic extinction).

The OII flux corresponds to a luminosity 4.31×10^{41} ergs s^{-1}, which from the relation of Kennicutt (1998), SFR $= 1.4 \times 10^{-41} \mathrm{L}_{\mathrm{[OII]}}$, gives the SFR as 6.03 ± 0.35 $M_\odot$yr^{-1}. With a correction for Galactic extinction, the [OII] luminosity would be about 5.0×10^{41} ergs s^{-1} and thus the corresponding SFR 7.0 ± 0.4 $M_\odot$yr^{-1}.

Kobulnicky et al. (2003) describe a method of estimating the metallicity of star-forming galaxies using emission-line equivalent widths. Following these authors, we correct for stellar absorption by adding 2Å to the observed equivalent width of Hβ. Our measurements then give the ratios log(EW R_{23}) $= 0.61 \pm 0.03$ and log(EW O_{32}) $= -0.37 \pm 0.04$, and from equation 3 of Kobulnicky et al. (2003) the metallicity $12 + \log(\mathrm{O/H}) = 8.757 \pm 0.030$. On the basis of the Allende Prieto, Lambert, & Asplund (2001) measurement of the solar oxygen abundance, $12 + \log(\mathrm{O/H}) = 8.69 \pm 0.05$, this is 1.17 ± 0.15 solar.

Higher luminosity is generally correlated with high metallicity, but with a large scatter. On a luminosity-metallicity plot, Arp 295b is well within the observed range of local galaxies. Compared to the fitted relation for local NFGS + K92 galaxies (Kobulnicky et al. 2003), it is slightly and marginally (0.8 ± 0.5 mag) above the mean B luminosity for its (O/H).

4. DIRECT IMAGING

Figure 2 shows our 6000s combined image of Arp 295b in E6690, which will include both the Hα line emission and 91Å of red continuum. We therefore express the photon counts in terms of a continuum magnitude m_{6690}, in the AB system ($m_{AB} = 48.60 - 2.5 \log f_\nu$).

Figure 3 shows a contour plot of the galaxy disk. Arp 295b is a disturbed and somewhat asymmetric galaxy. The bright, compact nucleus is surrounded

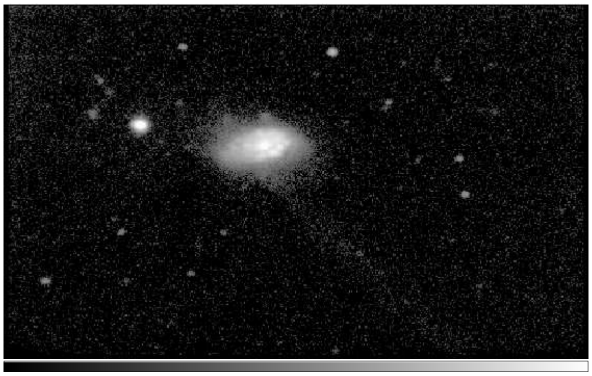

Fig. 2. Arp 295b imaged through the E6690 filter (6000s total); the area shown is 4.71×2.87 arcmin, N at the top and E at the left, with a log intensity scale.

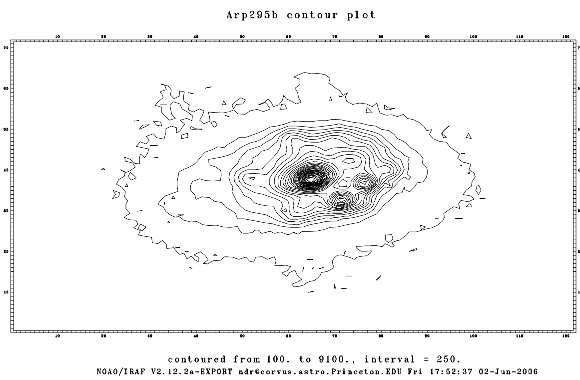

Fig. 3. Contour plot of the disk of Arp 295b, showing a 75×44 arcsec area. The min and max contours correspond to intensities 22.64 and 17.84 mag arcsec^{-2} in m_{6690}.

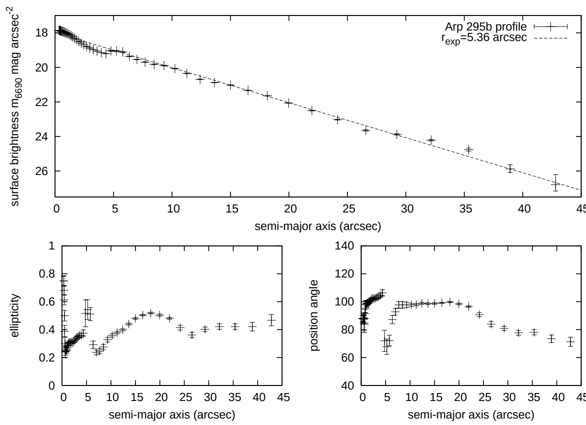

Fig. 4. Parameters of elliptical isophotes fit to Arp 295b, observed in E6690: surface brightness against semi-major axis (points) and best-fitting exponential (straight line); ellipticity, and position angle (in degrees anticlockwise from the North).

by at least 8 bright knots, presumably Hα emitting star-forming regions. The majority, and the brightest, of the knots are on the western side of the galaxy, up to 8 arcsec from the nucleus. However, the disk itself extends further to the east side of the nucleus, in the direction of the gaseous plume. Figure 2 also shows, faintly, the bridge extending SW towards Arp 295a, and two diffuse extensions north of the disk which appear to be the 'ring-shaped' Hα emission seen by Dopita et al. (2002).

To characterize the structure of the galaxy, we use IRAF 'isophot.ellipse' to fit the E6690 image with concentric elliptical isophotes. Figure 4 shows isophote surface brightness (SB), ellipticity and position angle (PA) as a function of semi-major axis (r_{sm}). These parameters fluctuate in the central $r \leq$ 7 arcsec because of 'knots', but the galaxy as a whole has an approximately exponential intensity profile with a best-fitting scalelength $r_{exp} = 5.36 \pm 0.55$ arcsec (2.52 ± 0.26 kpc). The ellipticity is consistent with the ~ 0.43 expected for the inclination of 55° (1-cos 55° = 0.43).

The position angle is $\sim 100°$ for the galaxy disk, shifting to 80° in the outermost isophotes where the isophotes follow the plume extending E of the disk. At no radius do we find a PA as far from E-W as the 112°.5 long-slit position used by Stockton (1974). The disk itself may be just slightly warped, its mean PA twisting from 103°.5 at $r < 5$ arcsec to 98°.3 at 10–20 arcsec.

The total flux from Arp 295b in this passband, integrating out to 39 arcsec, is $m_{6690} = 12.91$. The two UV-bright clumps reported by Neff et al. (2005) are visible but very faint. For 'clump 1', 86 arcsec east of the nucleus, $m_{6690} = 19.41$, and for 'clump 2', 16 arcsec to its north, $m_{6690} = 19.32$.

Figure 5 shows Arp 295a in E6690. Also visible is a smaller, round, galaxy 65 arcsec NW (position angle −59°) from 295a, at RA $23^h41^m43^s.9$, Dec -03:39:29. On the basis that this is probably a third galaxy in the system (which we will be able to confirm below, using MES), we refer to it hereafter as Arp 295c.

Using 'isophot' we fit isophotes to both galaxies (Figure 6). Arp 295a, integrated out to 49 arcsec, has a total magnitude $m_{6690} = 13.22$. The nucleus produces a central peak in the intensity plot, but at $5 < r < 50$ arcsec it is close to exponential with a best-fitting $r_{exp} = 11.16$ arcsec, or 5.24 kpc. The ellipticity is very high, as expected for the $\sim 85°$

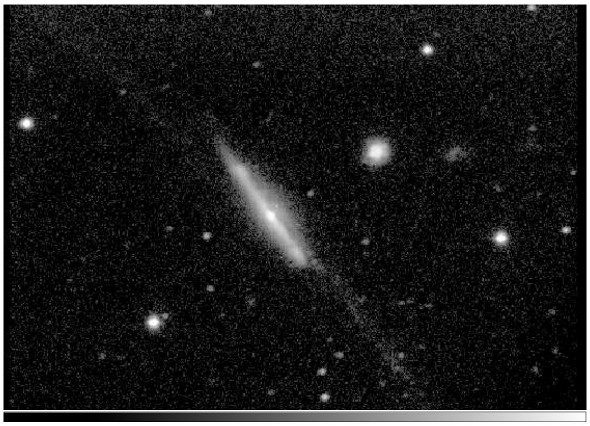

Fig. 5. Image centred on Arp 295a, E6690 filter (1200s); the area shown is 4.97×3.73 arcmin, N top and E left, with a log intensity scale.

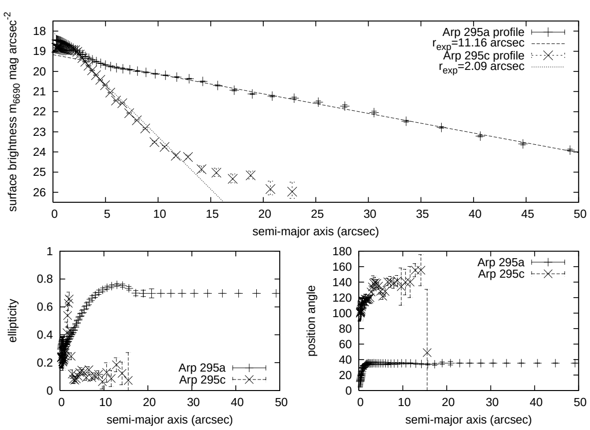

Fig. 6. Parameters of elliptical isophotes fit to Arp 295a and c, observed in E6690: surface brightness against semi-major axis (points) and best-fitting exponential (straight line); ellipticity, and position angle (in degrees anticlockwise from the North).

inclination, and the position angle about 35°, consistent with the 37° used by Stockton (1974).

Arp 295c, integrated out to 23 arcsec, has a total magnitude $m_{6690} = 14.65$. The intensity profile shows an excess above an exponential at $r > 12$ arcsec, and is too flat in the centre for either an exponential or a de Vaucouleurs profile. The nucleus appears either double-peaked or barred, hence elongated, but at all larger radii the ellipticity is very low ~ 0.1. The half-light radius r_{hl} is 3.35 arcsec (1.57 kpc), and fitting an exponential to the steep part of the profile, $2 < r < 14$ arcsec, gives $r_{exp} = 2.09$ arscec, or 0.98 kpc. The form of the intensity profile, the appearance and the scalelength of Arp 295c

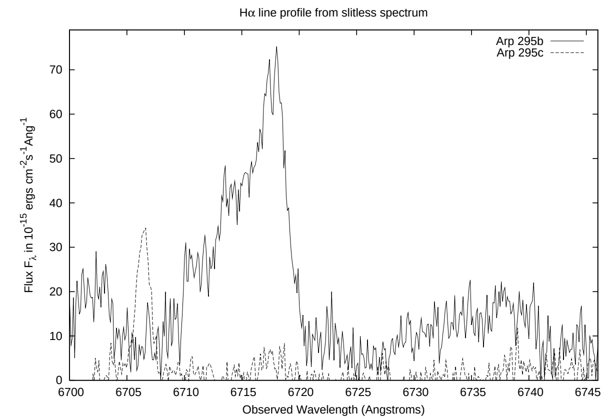

Fig. 7. MES spectra in the Hα line region for the spiral Arp 295b and the irregular Arp 295c, obtained from slitless observations so as to include the entire flux from each galaxy.

indicate it is probably an Im type (e.g. Hunter & Elmegreen 2006).

5. Hα FLUX FROM SLITLESS SPECTRA

To measure the Hα line flux from each galaxy, separate from the continuum, we take *slitless* spectra with MES in spectroscopic mode (grating rather than mirror). Single exposures of 1200 sec were taken on both the Arp 295b and Arp295a/c fields. If a galaxy is a Hα emitter, these images will show the Hα line, extended in the spatial axis but also smeared out in the dispersion axis due to the extension of the galaxy. Because no slit was used the images will contain the entire Hα flux from all parts of the galaxy.

We see strong Hα line emission for Arp 295b and 296c, (confirming that 295c is equidistant, thus physically associated with the spirals). However, we see no emission line for 295a, so its brightness on the E6690 direct-image must have been due to its red continuum. For 295b/c, we extract the Hα lines from their slitless spectra, using 'apall' with wide extraction apertures that encompass all the emission.

Because the galaxies are extended, wavelength calibration will inevitably be less precise when spectra are taken without slits. Our slitless exposure of Arp 295b was taken immediately following an exposure through the slit, without moving the telescope. In this exposure the slit was 5.77 arcsec north of the galaxy centre, so to correct for this we apply a correction −0.98Å to the slitless spectrum wavelength calibration. For our slitless spectrum of Arp 295c, the telescope was actually pointed at Arp 295a, and so we wavelength calibrate by matching the Hα line centroid to that measured on a separate exposure of Arp 295c where the slit was used and placed on the galaxy (to look for evidence of rotation). Following these corrections we flux calibrated using the slitless spectrum of 58 Aquilae. Figure 7 shows integrated Hα profiles, wavelength and flux calibrated. We measure the total Hα flux for each galaxy by integrating over the Hα line profile and subtracting the continuum (i.e. the mean flux in wavelength intervals on either side of the line), which gives for Arp 295b, 3.47×10^{-13} ergs $\mathrm{cm}^{-2}\mathrm{s}^{-1}$, corresponding to a luminosity 4.27×10^{41} ergs s^{-1}. With a 0.102 mag correction for Galactic extinction this increases to 3.72×10^{-13} ergs $\mathrm{cm}^{-2}\mathrm{s}^{-1}$ and 4.69×10^{41} ergs s^{-1}. We also estimate the restframe equivalent width of Hα as 45Å.

The centroid wavelength is 6715.61Å, which implies a redshift of 0.02328 or a velocity of 6980 km s^{-1}. This may be a small overestimate because the receding (west) side of this galaxy is the more strongly emitting. At the nucleus or kinematic centre of the galaxy the wavelength is closer to 6714.5Å, which implies a redshift of 0.02312 or a velocity of 6930 km s^{-1}.

We measure the Hα flux from the irregular Arp 295c as 5.00×10^{-14} ergs cm^{-2} s^{-1}, which corresponds to a luminosity 6.16×10^{40} ergs s^{-1}. With a 0.102 mag correction for Galactic extinction these increase to 5.49×10^{-13} ergs $\mathrm{cm}^{-2}\mathrm{s}^{-1}$ and 6.76×10^{40} ergs s^{-1}. The centroid wavelength is 6706.46Å, which implies a redshift of 0.02189 or a velocity of 6562 km s^{-1}. Note the high velocity of approach, almost 370 km s^{-1}, relative to Arp 295b. The radial velocity relative to Arp 295a, which it is much closer to, is 287 km s^{-1} (Arp 295a velocity from de Vaucouleurs et al. 1991).

6. KINEMATICS FROM Hα SLIT SPECTRA

Our high-resolution MES spectroscopy traces the mean line-of-sight velocity of the Hα emitting gas as a function of distance along the slit. With multiple slit positions a 2D velocity map can be built up.

For Arp 295b we took exposures at 9 slit positions on the galaxy disk, ranging from 8.027 pixels south to 9.308 pixels north of the nucleus, always with the slit aligned E-W (The slit positions were determined using the position of a star on the corresponding 'mirror-slit' images).

Each slit exposure was examined using IRAF 'splot' to find the centroid wavelength (λ_{obs}) for the peak of Hα emission, as a function of position along the slit. Using our wavelength calibration, this position is converted into a wavelength λ_obs and

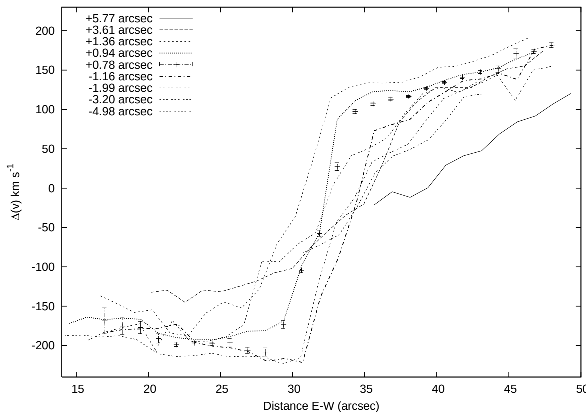

Fig. 8. Hα line velocity for Arp295b, in the rest-frame (relative to the approximate median recession velocity of 6930 km s^{-1}), as a function of distance from E to W along each slit position. The slit positions are denoted by arcsec N (or S if negative) of the galaxy nucleus. The central slit position's velocities are plotted as points with errorbars.

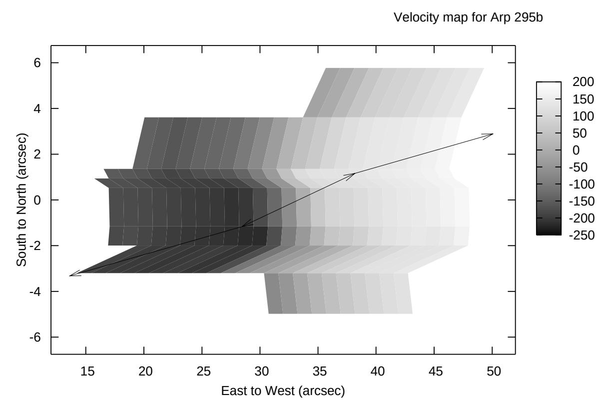

Fig. 9. Hα Velocity map for Arp295b in kms^{-1} of recession in the line-of-sight, relative to the nucleus (6930 km s^{-1}). The arrows show the approximate long axis of the disk.

then to a relative velocity in the galaxy rest-frame, $\Delta v = c(\lambda_{obs} - \lambda_0)/(1+z)\lambda_0$ where z is the centroid redshift of the galaxy (taken as $z = 0.02312$ for Arp 295b) and $\lambda_0 = 6252.8(1+z)$.

Figure 8 shows Δv against position on the E-W axis for the 9 slit positions, plotted as lines except for the slit position closest to the centre, where the velocity is plotted as points with errorbars (derived by 'splot') to show typical uncertainties. This shows that the east side of Arp 295b is approaching and the west receding, by ~ 200 km s^{-1}, and that there is a definite asymmetry in the velocity curves on the E and W sides of the galaxy, which is apparent at sev-

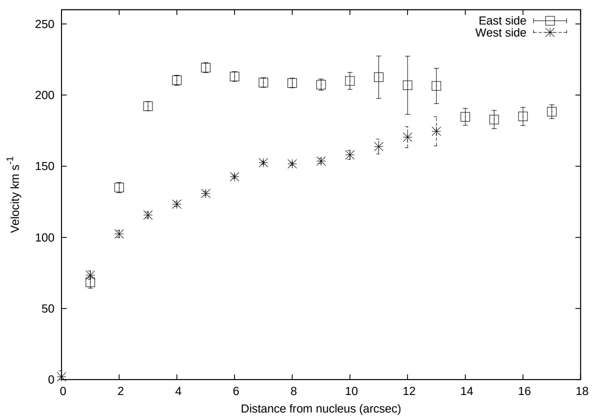

Fig. 10. Magnitude of the line-of-sight velocity extracted on the long axis of Arp295b (as depicted by the arrows on Figure 9), as a function of distance from the nucleus, shown separately for the east and west sides of the galaxy.

eral slit positions. The greatest difference between any two velocities in this plot is 413.8 ± 16.3 km s^{-1}. Dividing this by 2 sin 55° (the disk inclination), gives the maximum rotation velocity as 252.6 ± 9.9 km s^{-1}.

In addition to spectroscopy on the disk of Arp 295b, we take exposures with the slit placed across the nucleus and disk of Arp 295a, and on one of the candidate tidal dwarf galaxies of Neff et al. (2005). However, none of these showed any visible line emission. We also observe with the slit across Arp 295c. This does show emission, but we do not find any significant rotation; any velocity gradient across the disk is < 10 km s^{-1}. This implies its orientation is almost exactly face-on. There are two ways in which we can try to show the kinematics more clearly. The first is by generating a 2D velocity map (Figure 9). This shows how the greatest recession velocity is not at the eastern extreme but at a point intermediate between this and the nucleus, and that the rotation of the galaxy is inclined (by at least 10°) with respect to the E-W axis of our slits.

The second way is by extracting a rotation curve along the true long axis of the galaxy disk. To take into account the warping of the disk we represent this axis as a line passing though the centre with a PA of 103.5° at $r < 5$ arcsec, bending to a PA of 98.3° at larger radii (shown as the arrows on Figure 9). Along this locus, and separately in the east and west directions, we estimate the velocity by interpolating between the observed values on the adjacent slit positions. Figure 10 shows the velocity at 1 arcsec intervals, eastwards and westwards of the nucleus.

This shows clearly the asymmetry in the galaxy's rotation. On the west side the rotation curve rises slowly and monotonically; on the east side it rises more steeply but begins to turn over at $r = 5$ arcsec. At the smallest (~ 1 arcsec) and largest (~ 14 arcsec) radii the rotaion velocities are similar on the two sides but at intermediate radii, especially around 5 arcsec, the velocity is higher on the eastern (approaching) side, the difference reaching 88 km s^{-1} or a factor 1.675.

We can estimate a lower limit to the dynamical mass of Arp295b from the rotation velocity at the largest radius observed. The mass inwards of radius r is rv_{rot}^2/G. At 17 arcsec, which is 7.98 kpc, $v_{rot} = 188.3 \pm 4.8/(\sin 55°) = 229.9 \pm 5.9$ km s^{-1}, giving a mass within this radius $9.8 \times 10^{10} M_{\odot}$.

7. SUMMARY AND DISCUSSION

We have observed the Arp295 system of interacting galaxies, at $z = 0.0023$, using optical spectroscopy, imaging in a narrow (91Å) band centred on redshifted Hα, and high-resolution spectroscopy of the Hα line.

Arp 295a is an almost edge-on spiral for which we measure a scalelength $r_{exp} = 5.24$ kpc in red continuum. We did not detect Hα line emission with MES, either when the slit was placed on the galaxy, or when the galaxy was observed slitless.

Arp 295b is a spiral with a smaller scalelength $r_{exp} = 2.52$ kpc. Unlike its companion it is a strong source of Hα line emission and we measure a total Hα luminosity (corrected for Galactic extinction but not internal dust) of 4.69×10^{41} ergs s^{-1}. Our uncorrected measurement of the $H\alpha$ flux is similar to (10 per cent greater than) that given by Dopita et al. (2002). Our Hα luminosity estimate corresponds (from the relation of Kennicutt 1998) to a SFR of 3.7 $M_{\odot}$yr^{-1}.

Arp 295b is asymmetric, with the disk extending further from the nucleus on the east side (away from Arp 295a), where there is also an extended plume of neutral gas (e.g. Neff et al. 2005). There are bright knots of Hα emission concentrated around the nucleus and especially on its western side.

We obtained an optical spectrum of Arp 295b at 3600–5900Å, which showed emission lines of [OII]3727, [OIII]4959,5007, Hγ and Hβ, and absorption lines of H9, H(3968), MgI(5175) and Ca + Fe(5269).

From the emission line flux ratios and the formula of Kobulnicky et al. (2003) we estimate a metallicity $12 + \log(O/H) = 8.757 \pm 0.030$, approximately solar. This is consistent with the observed metallicity-luminosity relation of spiral galaxies – the luminosity is actually slightly (0.8 ± 0.5 mag) high for the (O/H). If this is significant it is presumably due to brightening from interaction-triggered star-formation.

The galaxy's [OII] emission is very strong (equivalent width 36Å) and if the slit spectrum is scaled to the total optical flux of the galaxy, the [OII] luminosity is 4.3 or 5.0×10^{41} ergs s^{-1} (without or with correction for Galactic extinction). However, on the basis of the Kennicutt (1998) relations, this corresponds to a SFR about twice that estimated from the Hα emission. It is possible that the slit sampled starbursting, presumably central, regions of the galaxy where the [OII] equivalent width was larger than for the galaxy as a whole, but it is also possible that the galaxy has a higher than average [OII]/Hα ratio.

The Kennicutt (1998) relation of SFR to $L_{[OII]}$ does include some dust extinction. Kewley, Geller, & Jansen (2004) have more recently estimated that if $L_{[OII]}$ is corrected for (or unaffected by) dust, the SFR$\times 6.58 \simeq 10^{-42} L_{[OII]}$. Hence, if Arp 295b suffers little internal dust extinction, both [OII] and Hα measures of SFR then give about 3.6 $M_\odot$ yr^{-1}. Furthermore, Kewley et al. (2004) find the intrinsic [OII]/Hα ratio to be dependent (non-monotonically) on the oxygen abundance. In the Kewley et al. (2004) relation, the [OII]/Hα $\simeq$ 0.94 we find is consistent with our abundance estimate, provided the internal dust extinction of Arp 295b is only $E(B-V) \simeq 0.1$–0.2 mag.

Two 'knots' in the eastern plume were claimed by Neff et al. (2005) to be formative tidal dwarf galaxies. On our direct imaging in E6690 we detected both objects, faintly ($R \sim 19$), but did not detect any Hα line emission with MES in spectroscopic mode, either by placing the MES slit on one knot or on a slitless observation of the whole field. Hence we could not determine whether or not these are genuine TDGs.

Our primary observation consists of a Hα velocity map of Arp 295b, built up by observing with MES at 9 slit positions from the north to the south edge of the galaxy disk. Arp 295b is rotating in the sense of receding on the western side, which is retrograde with respect to its orbit with Arp 295a. The maximum disk rotation velocity is estimated as 252.6 ± 9.9 km s^{-1} (consistent with the 245 km s^{-1} of Stockton 1974), and from the velocity 17 arcsec (7.98 kpc) from the nucleus we estimate the mass inward of this radius to be $9.8 \times 10^{10} M_\odot$.

Using the velocity map we determine the velocity curve on the long axis of the galaxy (taking into account that it is warped by a few degrees), and compare the kinematics of the east and west side of the galaxy. The rotation is very asymmetric. At the smallest and largest ($r > 14$ arcsec) radii, the rotation velocities are similar on both sides, but at intermediate radii, and most strongly at $r \sim 5$ arcsec (2.35 kpc), the rotation velocity is higher on the eastern (approaching) side by as much as 88 km s^{-1} in the line of sight, thus 107 km s^{-1} in true rotation velocity, or a factor 1.675.

We interpret this as a result of the asymmetry of the galaxy disk (Figures 2, 3), and hence of the gravitational potential, resulting from the tidal perturbation by the more massive Arp 295a. An asymmetry in the potential causes an relative asymmetry twice as great in the rotation curve (Jog 2002). Very close to the nucleus, the orbital kinematics will be dominated by the nucleus itself, so orbits are circular and symmetric. However, for larger orbits the effective centre of gravity is displaced eastwards of the nucleus, and so stars and gas orbiting the nucleus move faster while on the eastern side (simply by Kepler's laws). Here the asymmetry in the potential would peak at $\sim 4/3$ on a circle radius 5 arcsec about the nucleus. At the largest radii the velocities on the two sides tend to converge because the offset of the centre of mass becomes small compared to the orbital radius.

On the east side the velocity curve rises rapidly to $r = 5$ arcsec and beyond that is either flat or falls slightly. On the west side the velocity curve rises less steeply but monotonically to $r \simeq 13$ arcsec, and at $r \leq 7$ arcsec it approaches solid-body rotation. We saw (Figures 2 and 3) that the brightest star-forming, Hα luminous knots tended to concentrate on the west side of the nucleus, where they extend out to 7 or 8 arcsec. We hypothesize that the slowed or solid-body rotation on the western side of the nucleus locally enhances the star-formation and therefore causes the asymmetric distribution of these hotspots.

Keel (1993), examining a sample of interacting spirals, found an association between high star-formation rates and disturbed kinematics, in particular solid-body rotation and very slow rotation (caused by near-radial stellar orbits). These altered kinematics would lower the threshold for large-scale disk instabilities to develop, causing gas to flow inwards and triggering starbursting. Our findings for Arp 295b appear to support this model.

Of the two spirals, Arp 295a appears to be affected far less by the interaction, in that its disk is not obviously asymmetric and it is not starbursting.

While we cannot estimate the SFR of SArp 295a from our data, the far IR flux suggests its is an order of magnitude below that of the smaller spiral (Hibbard & van Gorkom 1996). The disturbed form of Arp 295b must result from the two galaxies having undergone a very close passage within the last few 10^8 years. There are three obvious reasons why the effect on Arp 295a was different.

Firstly, although Arp 295a is only 0.1 mag brighter than 295b in the B-band, this magnitude will be greatly affected by internal extinction due to its edge-on orientation. In the K band (2MASS 2003) where dust extinction is less efffective, Arp 295a (with $K = 10.09$) is the brighter by 0.65 mag. Similarly, Masters, Giovanalli, & Haynes (2003) estimated that edge-on spirals are typically dimmed by at least $\Delta(I) \simeq 0.9$ mag relative to their face-on magnitudes. As the difference in axis ratio between Arp 295a and 295b is about 0.4 and the B extinction will be about twice that in I, the real difference in their B luminosities would be $\sim 0.1+(0.4\times2\times0.9) = 0.82$ mag.

On this basis 295a is likely to be at least twice as massive as 295b (Stockton 1974 estimated an even higher mass ratio of 3.5, although may have underestimated the mass of 295b due to its asymmetric rotation curve). We also measure the disk scalelength of Arp 295a as larger by a factor of 2.08. The twofold or more mass difference means Arp 295a suffered substantially less tidal perturbation in the close passage. Furthermore, tidal effects within the disk of Arp 295a will be less apparent due to its edge-on orientation. And despite the mass difference, Arp 295a does show definite tidal effects at larger radii in the form of the long tail extending SW.

Secondly, according to the HI masses of Hibbard & van Gorkon (1996), Arp 295b has a greater gas content by a factor of 3.45, and this will be much more concentrated because the disk area is only about 0.23 times as great. On the basis of a SFR $\propto \rho^{1.4}$ Schmidt law (Kennicutt 1998), this already could account for a factor of $(3.45/0.23)^{1.4} \times 0.23 = 10$ in SFR. However, it is probable that the greater tidal disturbance of Arp 295b is also important, especially if, as in the 'shock-induced starformation' model of Barnes (2004), the local SFR is strongly dependent on the strength of tidal effects as well as on the gas density.

Thirdly, Arp 295a is rotating prograde with respect to the mutual orbit of the galaxies, while 295b is retrograde, although with a significant tilt from the orbital plane. This could explain why tidal effects in Arp 295a produced a long thin tidal tail, while in 295b a broad gas-rich plume was ejected, much as predicted by simulations (e.g. Barnes 1992) and previously observed (e.g. Hibbard & Yun 1999) for prograde-retrograde mergers.

We also investigate a third galaxy in the system, Arp 295c, situated 65 arcsec from Arp 295a. It is rounder and much smaller than the two spirals (and approximately 1.5 mag fainter), with a half-light radius 1.57 kpc. Its radial intensity profile differs from a pure exponential, being flatter in the centre and with an excess at large radii, consistent with an Im type. We detected no significant gradient of velocity across the galaxy, implying its rotation axis is close to the line of sight (and thus perpendicular to that of Arp 295a). It is Hα luminous with $L_{\mathrm{H}\alpha} = 6.76\times10^{40}$ ergs s^{-1} (corrected for Galactic extinction), which corresponds to a SFR of 0.53 $M_\odot$ yr^{-1}.

We measure the recession velocity of Arp295c as 6562 km s^{-1}, indicating a radial approach of 287 km s^{-1} relative to Arp 295a. Stockton (1974) found Arp 295a to have a high disk rotation velocity of 300 km s^{-1}. This implies that the high radial velocity of Arp 295c may be accounted for by its normal orbital rotation about the massive 295a, and is not necessarily a result of the interaction of the two spirals.

A search of the Caltech NED database revealed that a galaxy with strong ultraviolet was previously observed at the position of Arp 295c and named Markarian 0933 (Markarian, Lipovetskii, & Stepanian 1977; Kojoian, Elliot, & Tovmassian 1981). For this, Fouque et al. (1992) measured an optical line recession velocity of 6590 km s^{-1}, close to our measurement, and its K_s band magnitude (2MASS 2003) is $K_s = 13.10$, compared to $K_s = 10.09$ for Arp 295a and 10.74 for Arp 295b. It is thus a factor 8.8 fainter than Arp 295b in K_s, compared to a factor 6.8 in Hα, implying the ratios of SFR to old stellar mass are quite similar in the two galaxies. Gutiérrez et al. (2006) investigated the Hα emission from a large sample of close irregular companions of large spirals, in the same luminosity range as Arp 295c, and the Hα SFR of 0.53 $M_\odot$ yr^{-1} places Arp 295c above the median but near the mean level of activity for this class of galaxy. Hence it is not clear, without a detailed analysis of its spectrum, to what extent the SFR may have been boosted by the close passage of Arp 295b.

NR acknowledges the support of the Universidad Nacional Autónoma de México, and the help of all at the Observatorio Astronómico Nacional, San Pedro

Mártir, in particular the very competent telescope operation of Gabriel García, in the observations described here.

REFERENCES

Allende Prieto, C., Lambert, D., & Asplund, M. 2001, ApJ, 556, L63
Arp, H. 1966, ApJS, 14, 1
Barnes, J. E. 1992, ApJ, 393, 484
__________. 2004, MNRAS, 350, 798
Burstein, D., & Heiles, C. 1982, AJ, 87, 1165
de Vaucouleurs, G., de Vaucouleurs, A., Corwin, H. G. Jr., Buta, R. J., Paturel, G., & Fouque, P. 1991, Third Reference Catalogue of Bright Galaxies (New York: Springer-Verlag)
Dopita, M. A., Pereira, M., Kewley, L. J., & Capaccioli, M. 2002, ApJS, 143, 47
Fouque, P., Durand, N., Bottinelli, L., Gouguenheim, L., & Paturel, G. 1992, Catalogue of Optical Radial Velocities (Paris: Obs. Lyon, Paris-Meudon)
Gutiérrez, C. M., Alonso, M. S., Funes, J. G., & Ribeiro, M. B. 2006, AJ, 132, 596
Hamuy, M., Suntzeff, N. B., Heathcote, S. R., Walker, A. R., Gigoux, P., & Phillips, M. M. 1994, PASP, 106, 566
Hibbard, J. E., & van Gorkom, J. H. 1996, AJ, 111, 655
Hibbard, J. E., & Yun, M. S. 1999, AJ, 118, 162
Hunter, D. A., & Elmegreen, B. G. 2006, ApJS, 162, 49
Jog, C. J. 2002, A&A, 391, 471
Keel, W. C. 1993, AJ, 106, 1771
Kennicutt, R. C. 1998, ApJ, 498, 541
Kewley, L. J., Geller, M. J., & Jansen, R. A. 2004, AJ, 127, 2002
Kobulnicky, H. A., et al. 2003, ApJ, 599, 1006
Kojoian, G., Elliott, R., & Tovmassian, H. M. 1981, AJ, 86, 811
Markarian, B. E., Lipovetskii, V. A., & Stepanian, D. A. 1977, Astrofizika, 13, 225
Masters, K., Giovanelli, R., & Haynes, M. P. 2003, AJ, 126, 158
Meaburn, J. 2003, RevMexAA, 39, 185
Neff, S. G., et al. 2005, ApJ, 619, 91
Oke, J. B. 1990, AJ, 99, 162
Stockton, A. 1974, ApJ, 190, 47

Nathan Roche: Instituto de Astronomía, Universidad Nacional Autónoma de México, Apdo. Postal 3-72, 22860 Ensenada, B. C., Mexico. Now at South African Astronomical Observatory, P.O. Box 9, Observatory 7935, Cape Town, South Africa (roche@ukzn.ac.za).